International Conference on Applied Energy 2019
Aug 12-15, 2019, Västerås, Sweden
Paper ID: 1077

THERMODYNAMIC ASSESSMENT OF STEAM-ACCUMULATION THERMAL ENERGY STORAGE IN CONCENTRATING SOLAR POWER PLANTS

Abdullah A. Al Kindi[1], Antonio M. Pantaleo[1,2], Kai Wang[1], Christos N. Markides[1,*]
1 Clean Energy Processes (CEP) Laboratory, Department of Chemical Engineering, Imperial College London, London SW7 2AZ, United Kingdom
2 Department of Agro-environmental Sciences, University of Bari, Via Orabona 3, 70125 Bari, Italy
* Corresponding author. Tel.: +44 (0)20 7594 1601. E-mail address: c.markides@imperial.ac.uk

ABSTRACT

Concentrated Solar Power (CSP) plants are usually coupled with Thermal Energy Storage (TES) in order to increase the generation capacity and reduce energy output fluctuations and the levelized cost of the energy. In Direct Steam Generation (DSG) CSP plants, a popular TES option relies on steam accumulation. This conventional option, however, is constrained by temperature and pressure limits, and delivers saturated or slightly superheated steam at low pressure during discharge, which is undesirable for part-load turbine operation. However, steam accumulation can be integrated with sensible-heat storage in concrete to provide high-temperature superheated steam at higher pressures. The conventional steam accumulation option and the integrated concrete-steam option are presented, analysed and compared in this paper. The comparison shows that the integrated option provides more storage capacity by utilizing most of the available thermal power in the solar receiver. Further, the integrated option delivers higher power output with enhanced thermal efficiency for longer periods when the power plant is solely operating using the stored thermal energy. An application to the 50 MW Khi Solar One CSP plant, based on solar tower and in operation in South Africa, is proposed.

Keywords: renewable/green energy resources, advanced energy technologies, thermal energy storage.

NONMENCLATURE

Symbols	
ρ	Density [kg/m^3]
c_v	Specific heat capacity [J/kg·K]
k	Thermal conductivity [W/m·K]
P	Pressure [Pa]
T	Temperature [K]
Q	Heat [J]
$\dot{m}$	Mass flow rate [kg/s]
Subscripts	
C	Concrete
S	Steam

1. INTRODUCTION

Decarbonization in energy sector is pivotal in the transition to a low-carbon and sustainable future and solar energy can play a leading role in this process. One of the latest technologies of power generation from solar heat is Direct Steam Generation (DSG) solar power plants. In DSG, water is used not only as the heat transfer fluid (HTF) in the solar receivers but also as the working fluid in the thermodynamic power-cycle [1]. Using only one fluid eliminates the need of heat exchangers for transferring heat between the HTF and the working fluid, which is the case in most conventional Concentrated Solar Power (CSP) plants [2].

Most solar power plants are coupled with thermal energy storage (TES) systems that store excess heat during daytime and discharge during night [3]. In DSG plants, the typical TES options include: (i) direct steam accumulation, (ii) indirect sensible heat storage, and (iii) indirect latent heat storage [4]. Option (i) is considered as a direct method because the thermal energy is stored directly in the HTF. However, options (ii) and (iii) are indirect since the thermal energy is stored in another storage medium [4].

Steam accumulation is the simplest heat storage technology for DSG since steam is directly stored in a storage pressure vessel, i.e., steam accumulator, in form of pressurized saturated water [5]. Discharging from steam accumulators usually takes place from the top part of the vessel as it is filled with saturated steam at the saturation pressure. Steam accumulation is commercially available and was implemented in several operating DSG power plants, such as the PS10 plant in Spain, and the Khi Solar One plant in South Africa [6]. A major disadvantage of steam accumulation is its relatively low temperature of the outlet saturated steam, compared with normal DSG operating temperatures, which is constrained by the wall size and the material of the pressure vessel [7]. The low steam temperature is not desired since it decreases the cycle

Selection and peer-review under responsibility of the scientific committee of the 11th Int. Conf. on Applied Energy (ICAE2019).

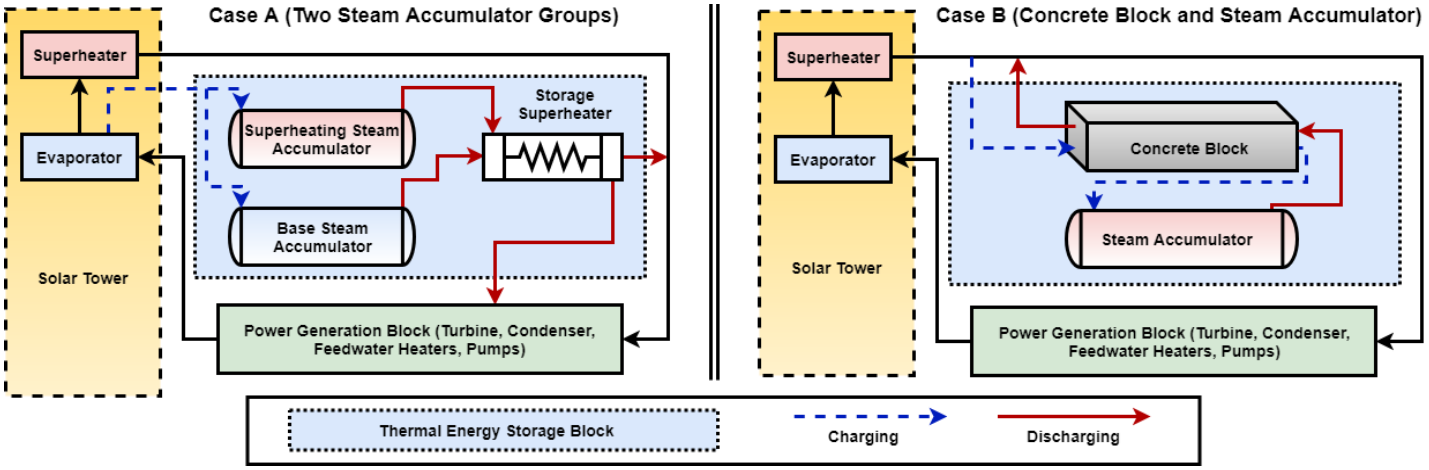

Figure 1 Schematic diagrams of the compared steam-accumulation TES options. Case-A (left): two steam accumulator groups, and Case-B (right) concrete block and steam accumulator.

thermal efficiency and it increases the risk of damaging the steam turbines at part loads operations [8]. Therefore, steam-accumulation TES systems in DSG are usually coupled with a superheater. There are two main options for superheating the saturated steam: (A) two groups of steam accumulators with a superheating heat exchanger and (B) one group of steam accumulator integrated with sensible or latent heat storage [5].

Prieto et al. [9] compared the thermodynamic and economic performance of the two above-mentioned superheating options, in which two-tanks of molten-salt are used for the superheating process in the extended configuration. It was concluded that the conventional option is more feasible and more cost effective than using steam accumulators and molten-salt combination for energy storage. This is mainly due to the complexity, high melting point and high costs of molten-salt storage systems. Further, Bai et al. [10] analysed the thermal characteristics of combining steam accumulators with concrete as superheating storage media. It was concluded that it is applicable to use this particular combination. However, the performance of this arrangement was not evaluated in a whole power plant cycle level and it was not compared to the first conventional superheating option. Moreover, several studies proposed and tested different sensible heat and latent TES configurations for DSG [6,11-13], but steam accumulators were completely removed in those TES configurations.

There are many options for solid-state sensible heat storage to be considered in the second option. These include concrete, cast iron, cast steel, silica fire bricks, etc. However, concrete has proven, through testing, its capability of high-temperature heat storage (up to 500 ˚C), its ability to withstand large number of charging/discharging cycles, and its relatively low cost [14-17].

The aim of this work is to perform a thermodynamic analysis and comparison of the two steam-accumulation options for a DSG power plant during charging and discharging modes. Concrete is considered for high-temperature sensible heat storage in the second option. In Section 2, the TES configurations and the modelling methodology are briefly described. The thermodynamic evaluations of the two configurations are presented in Section 3. Finally, the key findings from this study are summarized in Section 4.

2. METHODOLOGY

2.1 Description of the Reference DSG CSP Plant

Khi Solar One (KSO), which is a DSG solar tower CSP plant in South Africa, is selected as the reference plant in this study. The main components of the KSO plant are: a heliostat field, a solar tower that comprises of two solar receivers (an evaporator and a superheater), a steam turbine, a condenser, two feedwater pumps, three feedwater heaters, and a thermal energy storage system. The solar tower is designed to absorb a maximum solar heat of 243 MWt, in which part of this heat is utilized for generating 50 MW of electric power while the remaining heat can be stored in the TES system.

The comparative study between the two steam accumulation systems is performed using the same solar heat input and, the same total number of steam accumulators (i.e. same total volume), and the same power generation components. Figure 1 shows the schematic diagrams of the compared steam accumulation TES systems. Case-A is the conventional steam accumulation system used in KSO, which consists of two groups of steam

accumulators (superheating and base) and a storage superheater. Case-B is the extended storage system, which includes concrete blocks and same number of steam accumulators. The steam Rankine cycle for both cases is numerically modelled using MATLAB and all steam properties are provided by REFPROP.

2.1.1 Case-A (Two Steam Accumulator Groups)

During charging mode, feedwater flows into the evaporator and absorbs heat until becoming saturated steam at 12.3 MPa. Some amount of the saturated steam is fed into the two groups of the steam accumulators for storage, while the rest flows into the solar superheater to get superheated to 530 ˚C at 12.0 MPa. The superheated steam is then used to drive the steam turbine to generate electrical power. In Case-A, the superheating steam accumulators (SSA) are charged first, then the base steam accumulators (BSA) are filled. The charging process is terminated when the pressure of the steam accumulators has reached its maximum. The superheating group are always charged to higher pressure and temperature levels, compared to those in the base group. This is due to the need of higher temperature steam for the superheating process in the discharging mode.

During the discharge mode, base steam accumulators discharges saturated steam at the stored pressure. This steam flows through the storage superheater, gets superheated using higher temperature steam from the superheating steam accumulators, and then flows into the steam turbine to generate electricity. Superheating is essential to avoid creation of water droplets in the steam turbine as well as to increase the cycle thermal efficiency.

2.1.2 Case-B (Concrete Blocks and Steam Accumulators)

In Case-B, the same total thermal power from the solar field, i.e., 243 MWt, is used to superheat both live steam for power generation and excess steam for storage. However, since the steam accumulators are designed to store saturated steam only, the superheated storage steam flowing through the concrete blocks initially deposits excess heat to the concrete blocks until it reaches saturated state, which is then stored in the steam accumulators (SA). The charging mode takes place until the steam accumulators pressure reaches the desired point, which is assumed to be the same as the maximum pressure of the superheating group in Case-A. During the discharge mode, the stored steam flows back, in the opposite direction, through the heated concrete blocks and gets superheated before entering the steam turbine.

2.2 Steam Accumulator Model

All steam accumulators are thermodynamically modelled using the mass and the energy balance equations of the equilibrium model provided by Stevanovic et al. [18]. From Stevanovic et al. paper, the equations are solved numerically using Runge-Kutta methods to find the transient steam mass and pressure of the steam accumulator [18]. The volumes, initial water volume ratios, and initial and final pressures of the steam accumulators of both cases are indicated in Table 1. For Case-A, the maximum pressure values are selected to guarantee that there is sufficient heat from the superheating group to superheat the saturated steam during the discharging mode. The maximum pressure is selected based on the provided operating conditions of KSO. The minimum pressure of the base group is set at 1.4 MPa, which is based on the minimum steam turbine inlet pressure.

In Case-B, the minimum and the maximum pressure of all steam accumulators are 1.9 MPa and 8.2 MPa, respectively. The minimum is set by considering a 0.5 MPa pressure loss through the concrete blocks before entering the turbine. The maximum inlet steam temperature and pressure of all steam accumulators for both cases is 327 ˚C and 12 MPa, respectively. All other thermodynamic

Table 1 Charging and discharging steam accumulator main steam parameters for both storage configurations (Case-A and Case-B).

Parameter	**Case-A (Khi Solar One)**				**Case-B (Extended Storage)**			
	Superheating SA		Base SA		SA		Concrete	
	Charge	Discharge	Charge	Discharge	Charge	Discharge	Charge	Discharge
Steam accumulator [units]	3		16		19		-	
Steam accumulator useful volume/unit [m³]	197		197		197		-	
Initial water volume ratio [%]	0.44	0.50	0.64	0.80	0.65	0.95	-	-
Initial pressure [MPa]	8.20	3.90	4.00	1.40	1.90	8.20	-	-
Final pressure [MPa]	3.90	8.20	1.40	4.00	8.20	1.90	-	-
Inlet steam temperature [˚C]	327	-	327	-	281-327	-	530	210-296
Inlet steam pressure [MPa]	12.3	-	12.3	-	11.5	-	12.0	8.20-1.90
Outlet steam temperature [˚C]	-	296-249	-	252-195	-	296-210	281-327	413-368
Outlet steam pressure [MPa]	-	8.20-3.90	-	4.00-1.40	-	8.20-1.90	11.5	7.70-1.40
Mass flow rate [kg/s]	40.9	4.00-2.70	40.9	27.5	29.8	27.5	27.5	27.5

parameters (temperature, pressure, mass flow rates) of the charging and discharging modes for both configurations are summarized in Table 1. The external surface of all steam accumulators is assumed to be perfectly insulated, so there is no heat loss to the environment.

2.3 Solid (Concrete) Storage Model

The new component in Case-B is the concrete blocks. For this work, concrete is selected since it has proven its capability of high temperature sensible heat storage [14]. Figure 2 shows the scheme of piping bundle in the concrete blocks. It is assumed that the concrete temperature is uniform in the radial direction which is measured at the central point of the concrete section as shown in Figure 2.

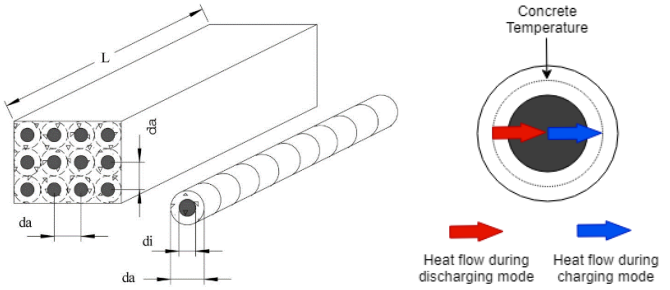

Figure 2 Schematic of piping bundle in the concrete block and the concrete temperature point.

The amount of heat and the final steam and concrete temperatures are calculated using Equations 1-4. These equations are solved by discretizing space (axial length) and time, same method used in Salomoni et al. [14]. It is assumed that there is no axial conduction in the concrete, and the external surface of concrete block is perfectly insulated, so there is no heat loss to the environment.

$$Q_{\mathrm{s}} = \dot{m}_{\mathrm{s}}\, c_{p,\mathrm{s}} \left(T_{\mathrm{s,out}} - T_{\mathrm{s,in}}\right) t \tag{1}$$

$$Q_{\mathrm{c}} = \mathrm{V}_{\mathrm{c}}\, \rho_{\mathrm{c}}\, c_{p,\mathrm{c}} \left(T_{\mathrm{c,fin}} - T_{\mathrm{c,init}}\right) \tag{2}$$

$$Q_{\mathrm{tran}} = UA \left(T_{\mathrm{s,avg}} - T_{\mathrm{c,avg}}\right) t \tag{3}$$

$$\frac{1}{UA} = \frac{1}{h_{\mathrm{s}} A_{\mathrm{t}}} + \frac{d_{\mathrm{c}}}{k_{\mathrm{c}} \overline{A_{\mathrm{c}}}} \tag{4}$$

where h_{s} is the heat transfer coefficient (HTC) of steam in W/m²·K from the Dittus-Boelter correlation [19], U the overall HTC in W/m²·K, A_{t} the tube surface area in m², d_{c} the concrete thickness in m, k_{c} the concrete thermal conductivity in W/m·K, $\overline{A_{\mathrm{c}}}$ the concrete mean surface area in m², V_{c} the concrete volume in m³, and t is time.

Table 2 summarizes the main parameters and dimensions of the concrete storage blocks. The concrete initial temperature before charging is 280 ˚C, which is selected assuming that the concrete blocks are heated after several charging/discharging cycles before performing this analysis.

Table 2 Concrete storage parameters

Parameter	Unit	Value
Number of concrete blocks	#	20.00
Concrete block length (L)	m	20.00
Number of tubes	#	10000
Tube diameter (di)	m	0.025
Concrete diameter (da)	m	0.040
Concrete average (ρ) [14]	kg/m³	2660
Concrete average (C_p) [14]	J/kg·K	800.0
Concrete average (k) [14]	W/m·K	2.000
Initial concrete (T) before charging	˚C	280.0
Pressure loss	MPa	0.025

3. RESULTS AND DISCUSSION

3.1 Charging Mode

The charging mode analysis is performed using the maximum thermal energy input of 243 MWt in both cases. About 60% of this heat is required for generating 50 MWe while the rest can be stored for night power generation. In this analysis, the 243 MWt solar heat is assumed to be available for at least 5 hours during the daytime. Specifically, the total thermal energy for these 5 hours is 1215 MWh, in which 730 MWh is required for maximum power generation while 485 MWh is available for storage.

The behaviour of the steam accumulators' pressure and the amount of stored energy during the charging mode for both cases are compared in Figure 3(A) and Figure 3(B), respectively. These plots are obtained by keeping the storage systems in full charging mode until the pressure of their steam accumulators have reached its maximum.

In Case-A, the superheating steam accumulators are filled first until reaching a maximum pressure of 8.2 MPa, taking about 18 minutes with a charging mass flow rate of 40.9 kg/s. Then, the base group are charged with the same mass flow rate for about 116 minutes until reaching a maximum pressure of 4.0 MPa. Therefore, Case-A storage configuration takes about 134 minutes to fill and stores about 232 MWh of thermal energy as indicated in Figure 3(B). About 14% of the 232 MWh heat is stored in the superheating group. Case-A storage system is unable to utilize all available solar heat during the 5 hours since it has already reached its assigned maximum pressure. In particular, only 232 MWh (48% of the available heat for storage) is accumulated in Case-A.

In Case-B, the charging mode starts at a pressure of 1.9 MPa. It takes about 280 minutes to fully charge all the steam accumulators. The longer charging duration is due to two main reasons. First, all Case-B steam accumulators have a maximum pressure of 8.2 MPa, so they can store more steam. Second, the charging mass flow rate is lower

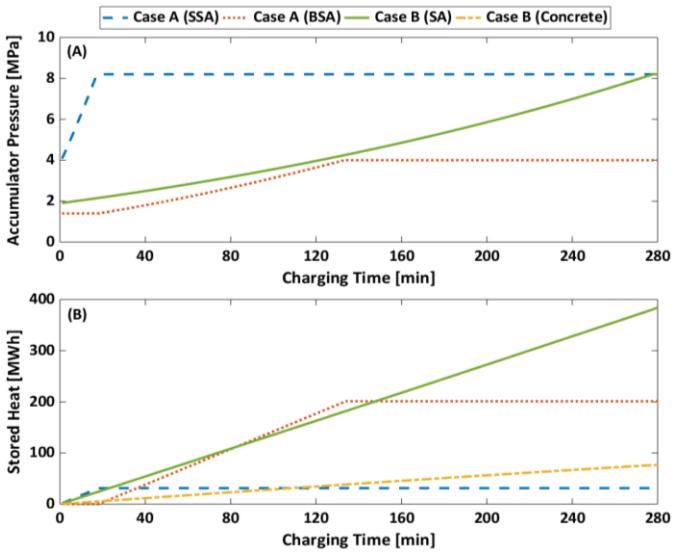

Figure 3 (A) Behaviour of steam accumulator pressure, and (B) amount of stored heat for both cases in charging mode.

in Case-B, which is 29.8 kg/s. It is lower since the storage steam is superheated to higher temperature, 530 ˚C, by absorbing the same amount of heat as Case-A. The total amount of heat stored in Case-B is 452 MWh, which is about 93% of all available heat for storage during the 5 hours period. This is expected since Case-B is charged for longer period. About 17% of the 452 MWh of stored heat is deposited in the concrete blocks, which is then used for the superheating process during discharge. Moreover, the highest temperature in Case-B is 470 ˚C. This temperature is located at the charging inlet of the concrete block. In contrast, the maximum temperature in Case-A storage configuration is 296 ˚C. The big temperature difference between the two configurations is because Case-B is charged with high temperature superheated steam, while Case-A is charged by saturated steam only.

Overall, Case-B takes longer time to charge but utilizes most of the available solar tower heat. Furthermore, Case-B has more heat storage capacity, about double the amount that of Case-A storage system. It should be mentioned that, according to our further analysis, even if Case-A is enlarged in order to have the same heat capacity as Case-B, it is not able to store heat at high temperatures as Case-B.

3.2 Discharging Mode

The discharging thermodynamic performance analysis for both cases is evaluated based on the generated power, its corresponding cycle thermal efficiency, discharging duration, and the total generated electricity. It is assumed that the discharging process starts immediately after charging for the Case-B. Therefore, the axial temperature profile of the concrete blocks stays fixed after the full charging process. Figure 4(A) compares the amount of generated power on the left y-axis and the total generated electricity on the right y-axis for both cases during night dischage. It should be mentioned that the power plant is operated only by the storage steam (i.e., no further steam input from the solar tower). Figure 4(B) shows the corresponding cycle thermal efficiency for each power level calculated using Equation 5. The discharging simulation results are obtained assuming that Case-A and Case-B are initially fully charged at their respective maximum pressure. The discharging mode is terminated when the turbine inlet steam pressure reaches the minimum allowable pressure of 1.4 MPa. These results are obtained using the identical steam inlet mass flow rate (27.5 kg/s), part-load turbine isentropic efficiency (85%), pump isentropic efficiency (75%), and turbine condensing pressure (0.016 MPa). It should be noted that the turbine efficiency is kept constant for all discharging loads.

$$\eta\,[\%] = \frac{P_{\text{out,net}}}{Q_{\text{in,stg}}} \times 100\% \qquad (5)$$

where η is the cycle thermal efficiency in [%], $P_{\text{out,net}}$ the net power generated by the power plant in MW, $Q_{\text{in,stg}}$ the thermal power input (MW) from the storage, calculated using, turbine mass flow rate, and the difference between storage outlet steam enthalpy and the ambient water enthalpy at (T_{amb} = 28 ˚C, P_{amb} = 0.1 MPa).

In Case-A, the discharging power starts at about 18 MWe with a cycle efficiency of 24%, whereas in Case-B it starts by generating 22.2 MWe with 27% of corresponding cycle efficiency. There is about 13% enhancement in cycle efficiency due to the increased turbine inlet pressure and temperature in Case-B. The Case-A turbine inlet pressure and temperature are 4 MPa and 252 ˚C, while in Case-B the pressure is 7.7 MPa and the

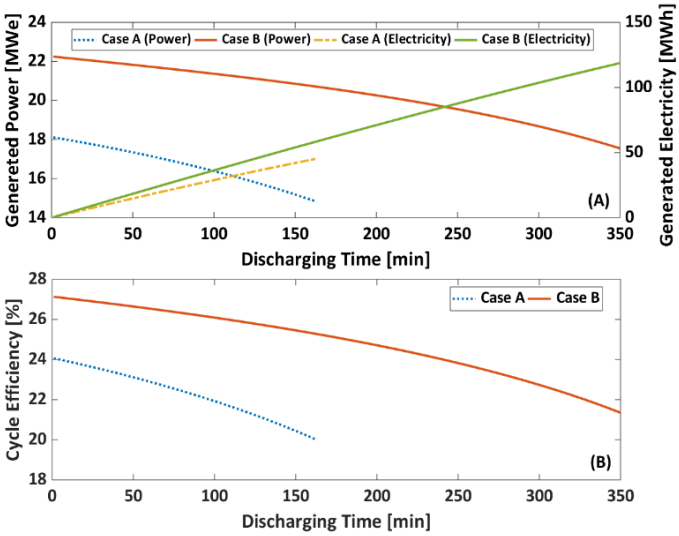

Figure 4 (A) Generated power and total generated electricity, and (B) The corresponding cycle thermal efficiency during discharging mode for the compared cases.

Table 3 Comparison of cycle performance for the same turbine inlet pressure

Parameter	Case-A	Case-B
Turbine inlet pressure [MPa]	4.00	4.00
Turbine inlet temperature [˚C]	252	385
Generated power [MWe]	18.0	20.2
Cycle efficiency [%]	24.0	25.0

temperature is 413 ˚C. The advanced superheating process of Case-B results in a higher thermal efficiency.

The performance of both cases is also compared for the same turbine inlet pressure of 4 MPa. The obtained simulation results at this pressure are summarized in Table 3. In Case-B, superheated steam flows into turbine at 385 ˚C, which increases the generated power by 12% and enhances the cycle efficiency by 4.5%, when compared to Case-B. The cycle efficiency for both cases is decreasing with time. This behaviour is expected since the inlet turbine pressure and temperature are decreasing with time.

The discharging duration for Case-A is about 160 minutes, generating a total electricity of 45 MWh. In the other hand, the discharging duration of Case-B is 350 minutes with a total electricity generation of 118 MWh. This is mainly due to the increased heat storage capacity of Case-B by the integration of concrete storage.

Overall, Case-B configuration, with the same steam accumulator volume of Case-A, delivers more power with an enhanced cycle efficiency for a longer duration at night.

4. CONCLUSION

This paper compared two steam accumulating TES solutions (cases) in DSG power plants: (A) two groups of steam accumulators and a superheater, and (B) one group of steam accumulators and concrete blocks for higher-temperature storage. The two configurations were thermodynamically compared under the same total solar tower thermal power input during 5 hours of charging time. Additionally, the two cases were analysed during discharge, in which the heat input was solely from the stored thermal energy. Case-B was able to store almost all available excess thermal energy during the 5 hours of charging (about 93% of available heat for storage), using the same total steam accumulator volume as Case-A. Furthermore, the maximum temperature of the stored heat is higher in Case-B after charging. The discharging mode analysis concluded that Case-B was capable of delivering higher power levels with improved cycle thermal efficiencies for longer (night-time) operation – about double the time of Case-A. This is mainly due to the Case-B's ability of storing heat at higher temperature. Future work includes: enhancement of concrete modelling and assumptions, optimisation of the concrete storage size and tube configuration, cost analysis for the two cases, and optimisation of storage capacity based on energy balances and profitability.

ACKNOWLEDGEMENTS

This research was funded by DFID through the Royal Society-DFID Africa Capacity Building Initiative.

REFERENCES

[1] Hirsch T, Feldhoff JF, Hennecke K, Pitz-Paal R. Advancements in the field of direct steam generation in linear solar concentrators-a review. Heat Transf Eng 2014;35:258–271.

[2] Birnbaum J, Eck M, Fichtner M, Hirsch T et al. A direct steam generation solar power plant with integrated thermal storage. 2010.

[3] Sarbu I, Sebarchievici C. A comprehensive review of thermal energy storage. Sustain 2018;10.

[4] Dirker J, Juggurnath D, Kaya A, Osowade EA et al. Thermal energy processes in direct steam generation solar systems: boiling, condensation and energy storage. Front Energy Res 2019;6.

[5] Steinmann WD, Eck M. Buffer storage for direct steam generation. Sol Energy 2006;80:1277–1282.

[6] González-Roubaud E., Pérez-Osorio D, Prieto C. Review of commercial thermal energy storage in concentrated solar power plants: Steam vs. molten salts. Renew Sustain Energy Rev 2017;80:133–148.

[7] Laing D, Bahl C, Fiß M, Hempel M et al. Combined storage system developments for direct steam generation in solar thermal power plants. 2016.

[8] Karakurt AS. Performance analysis of a steam turbine power plant at part load conditions. J Therm Eng 2017;3:1121–1121.

[9] Prieto C, Rodríguez A, Patiño D, Cabeza LF. Thermal energy storage evaluation in direct steam generation solar plants. Sol Energy 2018;159:501–509.

[10] Bai F, Xu C. Performance analysis of a two-stage thermal energy storage system using concrete and steam accumulator. Appl Therm Eng 2011;31:2764–2771.

[11] Seitz M, Cetin P, Eck M. Thermal storage concept for solar thermal power plants with direct steam generation. Energy Procedia 2013;49:993–1002.

[12] Valenzuela L. Thermal energy storage concepts for direct steam generation (DSG) solar plants, Adv Conc Sol Therm Res Technol 2016;269–289.

[13] Bachelier C, Selig M, Martins M, Steiglitz R et al. Systematic analysis of Fresnel CSP plants with energy storage. Energy Procedia 2015;69:1201–1210.

[14] Salomoni VA, Majorana CE, Giannuzzi GM, Miliozzi A et al.. Thermal storage of sensible heat using concrete modules in solar power plants. Sol Energy 2014;103:303–315.

[15] Laing D, Bahl C, Bauer T, Fiss M et al. High-temperature solid-media thermal energy storage for solar thermal power plants. Proc IEEE 2012;100:516–524.

[16] Laing D, Bauer T, Lehmann D, Bahl C. Development of a thermal energy storage system for parabolic trough power plants with direct steam generation. ASME 2009 3rd Int Conf Energy Sustain 2009;132:551–559.

[17] Eck M, Eickhoff M, Fontela P, Laing D et al. Test and demonstration of the Direct Steam Generation (DSG) at 500°C. SolarPaces Conf 2009.

[18] Stevanovic VD, Petrovic MM, Milivojevic S, Maslovaric B. Prediction and control of steam accumulation. Heat Transf Eng 2015;36:498–510.

[19] Purbolaksono J, Ahmed J, Khinani A, Ali A et al. (2009). Failure case studies of SA213-T22 steel tubes of boiler through computer simulations. J Loss Prev in the Proc Ind 2009;22:719-726.